Tetraheme Cytochrome *c* Subunit of *Rhodopseudomonas viridis* Characterized by EPR

Wolfgang Nitschke* and A. William Rutherford‡

Service de Biophysique, Département de Biologie, CEN Saclay, 91191 Gif sur Yvette Cedex, France

Received September 13, 1988; Revised Manuscript Received December 1, 1988

ABSTRACT: EPR signals of low-spin ferricytochrome hemes are described in membranes and reaction centers of the purple bacterium *Rhodopseudomonas viridis*. These are ascribed to the four hemes in the cytochrome *c* subunit of the reaction center, the structure of which has been solved by X-ray crystallography. We have addressed the question of the order of the hemes using several approaches. Redox potentiometry allows four hemes to be defined with E_m values of +400, +320, +20, and −80 mV. These hemes can be distinguished from each other by the spectral position of the g_z peak (g_z = 3.09, g_z > 3.32, g_z = 3.31, and g_z = 3.29, respectively) and by their relative orientation dependence in ordered membrane multilayers (90°, 45°, 45°, and 90° heme plane vs the membrane plane). In the fully reduced protein, low-temperature illumination leads to the specific oxidation of one heme which is probably the +20-mV heme. Warming in the dark results in the reduction of the photooxidized heme by the −80-mV heme. This indicates that the −80-mV heme is further from the reaction center than the heme oxidized at helium temperature. From these observations and from the crystal structure, we can eliminate 14 of the 16 heme arrangements. The remaining two models are as follows: (1) RC +400, +320, +20, and −80 mV; (2) RC +400, +20, +320, −80 mV. On the basis of a relaxation study of the hemes (which shows the lack of interaction between the +20- and −80-mV hemes but also what can be interpreted as a marked interaction between the +320-mV and either or both of the +20- and −80-mV hemes), we favor model 2. Other observations can be accommodated in this model.

When the three-dimensional structure of the bacterial reaction center was solved (Deisenhofer et al., 1984), the biggest surprise was the organization of the four hemes in the cytochrome subunit. The hemes were found to be arranged linearly in a protein subunit protruding from the membrane-spanning region at an angle into the aqueous phase. Although at that time the cytochrome had received little attention in *Rhodopseudomonas viridis*, the species crystallized, all of the evidence indicated close similarities to the bound cytochrome of other species of bacteria (Dutton & Prince, 1978). The hemes of the bound cytochrome act as electron donors to the photooxidized special bacteriochlorophyll (BChl)[1] pair of the photosynthetic reaction center. The oxidized hemes are themselves probably reduced by soluble cytochrome c_2 located in the periplasm (Shill & Wood, 1984). In some species, the bound cytochrome subunit is absent, and cytochrome c_2 donates directly to the special bacteriochlorophyll pair. Of the species containing the bound cytochromes, *Chromatium vinosum* was the best characterized spectroscopically prior to the crystallization of the *Rps. viridis* reaction center. In *C. vinosum*, four hemes are present, two high-potential and two low-potential hemes. The low-potential hemes are capable of donating electrons at low temperature while the high-potential hemes cannot (Dutton, 1971; DeVault & Chance, 1966). At room temperature, the low-potential hemes, when reduced in the dark, are photooxidized more rapidly than the high-potential hemes (Seibert & DeVault, 1970). Detailed EPR studies of the hemes showed that the high-potential hemes were perpendicular and the low-potential hemes were parallel to the membrane and that the distance between the two high-potential hemes and between the two low-potential hemes was greater than between the low- and the high-potential hemes (Tiede et al., 1978). Electrochromism indicated that the high-potential hemes were close to the outside of the membrane while the low-potential hemes were within the membrane (Case & Parson, 1973). An overall picture of the hemes in *C. vinosum* was established which was considered applicable to other species, especially since in all species investigated, the cytochromes, when present, had similar temperature, kinetic, and redox characteristics (Tiede et al., 1978).

The crystal structure changed all that and raised a number of interesting questions. The most obvious question is the following: What is the order of the hemes in the linear arrangement? This is a nontrivial question because of the contradictory structural requirements. The ability of the low-potential cytochromes to donate at low temperature, taken with their more rapid oxidation kinetics, might reasonably indicate they are closer to the reaction center than are the high-potential cytochromes. Yet in redox terms the interposition of low-potential cytochromes between the reaction center and the high-potential cytochromes in a linear arrangement would certainly not be predicted.

Since the crystal structure of the *Rps. viridis* reaction center was published, much more attention had been focused on the hemes in this species. Better resolved absorption spectra have been obtained, and specific spectral features attributed to each of the four hemes have been defined. Kinetic studies have shown rapid oxidation of the highest potential heme ($t_{1/2}$ = 0.32 μs) followed by slower ($t_{1/2}$ = 2.5 μs) heme to heme electron transfer from the second high-potential heme, indicating sequential electron transfer with the highest potential heme being closer to the reaction center (Dracheva et al., 1986, 1988; Shopes et al., 1987). This notion was further substantiated by comparison of the electrogenic phases due to the two individual electron-transfer steps (Skulachev et al., 1987;

‡Supported by the CNRS.

[1] Abbreviations: RC, reaction center complex; BChl, bacteriochlorophyll.

0006-2960/89/0428-3161$01.50/0

Dracheva et al., 1988). More precise redox titrations have defined separate midpoint potentials for each of the four hemes (Dracheva et al., 1986; Alegria & Dutton, 1987).

The hemes in *Rps. viridis* have until now received scant attention in EPR studies (Prince et al., 1978; Rutherford, 1979). In this paper, EPR signals from the hemes are identified and characterized in terms of their redox, relaxation, orientation, and electron-transfer properties. From a comparison with the data from X-ray crystallography (Deisenhofer et al., 1984), we arrived at a single preferred arrangement. Some of these results have appeared in a preliminary form elsewhere (Nitschke & Rutherford, 1988).

Experimental Procedures

Cultures of *Rps. viridis* were grown according to Cohen-Bazire et al. (1957) and chromatophore membranes were isolated by passing through a French press followed by centrifugation steps to remove soluble components and cell debris. Reaction centers were prepared as described by Clayton and Clayton (1978).

Redox poising and redox titrations of chromatophores (in 20 mM MOPS, pH 7.0, and at an ΔA_{1020nm} of approximately 200) were performed in near darkness under an appropriate safelight essentially as described by Dutton (1971). For some titrations, chromatophores were suspended in 2 mM ferricyanide/20 mM MOPS, pH 7.0, to oxidize the hemes and then washed 3 times, pelleted, and resuspended in 20 mM MOPS, pH 7.0, to remove excess ferricyanide. The following redox mediators were used: indigodisulfonate, indigotetrasulfonate, 2,5-dihydroxy-*p*-benzoquinone, pyocyanine, duroquinone, benzoquinone, 2,6-dichlorophenolindophenol, diaminodurol, 1,4-naphthoquinone, *N,N,N′,N′*-tetramethyl-*p*-phenylenediamine, vitamin K_3, and methylene blue at 100 μM and phenazine methosulfate, phenazine ethosulfate, and ferricyanide at 50 μM. Reductive titrations were carried out using sodium dithionite, and oxidative titrations were done using porphyrexide.

Oriented membrane multilayers were obtained by using the technique of Blasie et al. (1978): chromatophore membranes in H_2O were dried in 90% humidity atmosphere for approximately 24 h in darkness at 4 °C. In these membranes, various redox states were achieved by applying solutions of redox chemicals (sodium ascorbate or sodium dithionite at a range of concentrations in 20 mM MOPS, pH 7.0) to the dried membranes followed by drying under a stream of argon gas in darkness.

EPR spectra were obtained by using a Bruker 200 X-band spectrometer fitted with an Oxford Instruments cryostat and temperature control system.

Illumination in the EPR cavity was carried out by using a 800-W tungsten projector providing 16 000 μE m^{-2} s^{-1} of white light at the EPR cavity window after being filtered through 2 cm of water and two Calflex filters (Balzers) to remove infrared radiation.

Results

Midpoint Potentials. Figure 1 shows the EPR signals from the g_z components of ferric hemes in *Rps. viridis* chromatophores poised at a series of redox potentials. In the most oxidized samples, signals with two clearly distinct g values are observed: a narrow signal at $g = 3.09$ and a broader signal around $g = 3.3$. As the potential was lowered, the signals decrease in intensity as the hemes become reduced. The first signal to disappear is that at $g = 3.09$ followed closely by a decrease in the intensity of the $g = 3.3$ signal. These effects occur upon lowering the potential from 470 to 180 mV. At lower potential, the remaining $g = 3.3$ signal disappears. These redox effects indicate that the two high-potential hemes have signals at $g = 3.09$ and $g = 3.3$ while it appears that both low-potential hemes exhibit signals at $g = 3.3$. This is substantiated by the full redox titration of the two signals as shown in Figure 2. The $g = 3.3$ peak titrates in as two clearly distinct waves. However, three independent lines of evidence suggest that the low-potential wave actually consists of two distinct redox species: (1) It shows roughly twice the amplitude of the high-potential wave. (2) A Nernst simulation assuming one component yields a bad fit to the data points (Figure 2, dashed line), whereas two components with differing redox potentials allow for a satisfactory fit. (3) The line position of the $g = 3.3$ line shifts by 3 mT to higher fields during this wave of reduction. Titration of the line position demonstrates that the shift is almost complete when the low-potential wave has been reduced by only 50%. The plot of the line position shows an inflection point at a potential of 30 mV which is reasonably close to the midpoint potential of 20 mV estimated from the Nernst simulation. Thus, three cytochromes with midpoint potentials of −80, +20, and +320 mV independently give rise to signals at $g \approx 3.3$. The close to equal intensities

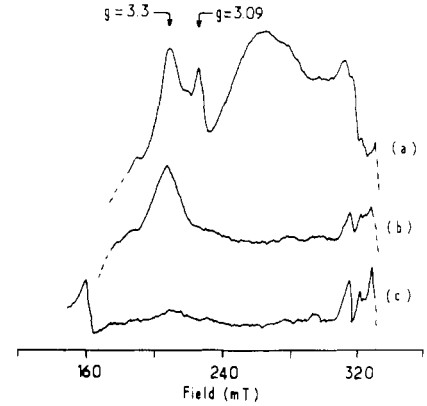

FIGURE 1: EPR spectra of *Rps. viridis* chromatophores poised at three different redox potentials as described under Experimental Procedures. (a) At 473 mV, all four cytochromes are oxidized; the broad band at about 250 mT is due to ferricyanide used as a mediator. (b) At 180 mV, only the two low-potential hemes at $g \approx 3.3$ remain oxidized. (c) Poising at −158 mV results in complete loss of low-spin signals. Instrument settings: temperature, 15 K; microwave power, 6.3 mW; frequency, 9.44 GHz; modulation amplitude, 3.2 mT; gain, 1×10^5.

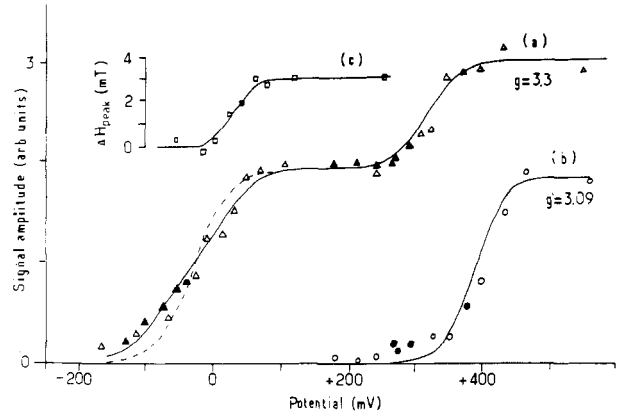

FIGURE 2: Redox titration of *Rps. viridis* chromatophores at pH 7.0. The signal size of the $g = 3.3$ peak (a) and the $g = 3.09$ peak (b) as well as the shift in field position of the $g = 3.3$ line (c) is plotted vs ambient potential (E_h). EPR spectra were obtained as described in the legend to Figure 1. Data points obtained on titrating in the negative and positive directions are denoted by open and closed symbols, respectively. For the case of the $g = 3.3$ peak, the Nernst simulation assuming two components is represented by a solid line, while the dashed line shows the one-component fit ($E_m = -20$ mV).

Table I: Relationship between Potentiometric, Spectral, Geometrical, and Functional Parameters of the Four Inequivalent Hemes

E_m (mV)	EPR signals g_z	EPR signals g_y	orientation (deg) (tilt of heme to membrane)	photooxidation at cryogenic temp	wavelength of α peak[a] (nm)
−80	3.29		90	yes (after warming)	554
+20	3.31		45	yes (5 K)	552
+320	>3.32		45	no	556
+400	3.09	2.23	90	no	559/552

[a] Data from Dracheva et al. (1988) correlated on the basis of the determined midpoint potentials.

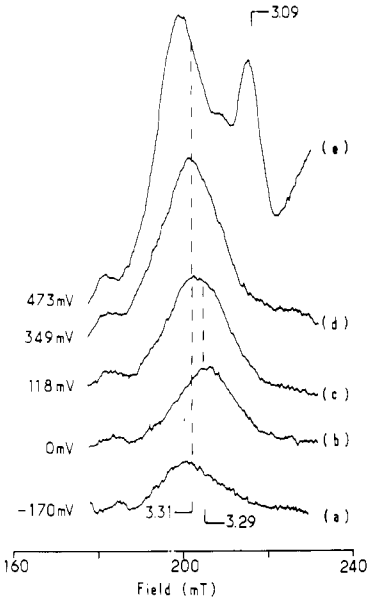

FIGURE 3: Comparison of the heme g_z peak positions observed under different conditions. (a) Photooxidized peak induced in a fully reduced sample (at −170 mV) by illumination at 4 K for 5 min. (b–d) g_z peaks of samples having one to four hemes oxidized. EPR conditions were as described in Figure 1.

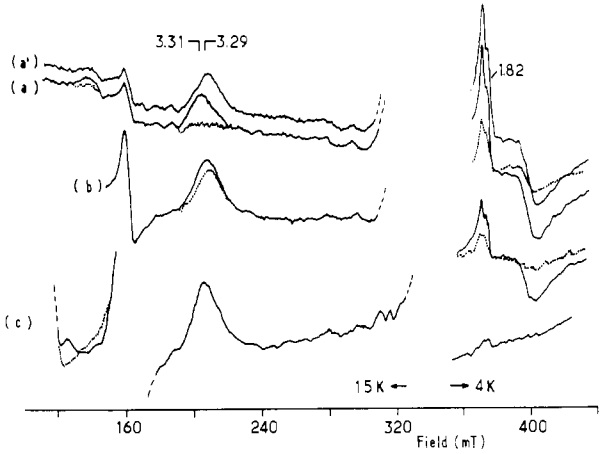

FIGURE 4: Spectral changes upon illumination at 4 K of samples poised at three different ambient potentials. (a) Samples poised at −200 mV. Photooxidation of a peak at $g = 3.31$ is accompanied by an increase in the semiquinone iron signal. (a′) After warming sample (a) to 100 K in the dark for 1 min, the peak has shifted to $g = 3.29$, whereas no significant change in the semiquinone iron signal can be observed. (b) Sample poised at 0 mV: 5-min illumination at 4 K results in an increase in peak height accompanied by a shift toward lower magnetic field. Again, these changes in the cytochrome region correlate with an increase in the semiquinone iron signal. No further changes occur on warming as in (a′) (spectra not shown). (c) Samples poised at 214 mV: no further oxidation of low-spin heme is observable; however, the appearance of a peak at $g \approx 5.4$ is evident. No spectral changes in the region of the semiquinone iron occur. For all cases, dotted lines denote spectra prior to illumination. In (a) and (b), illumination was carried out by 10 periods of 30-s light each followed by 30 s of darkness. This was to avoid heating of the sample. Prolonged or continuous illumination resulted in equivalent spectral changes. In (c), the sample was continuously illuminated at 4 K for 24 min; however, the same spectral changes were already observed by illumination following the protocol of (a) and (b). EPR conditions for the spectra at lower fields are as described in Figure 1, whereas for the higher field part (i.e., the semiquinone iron region) they were as follows: temperature, 4K; microwave power, 31 mW; frequency, 9.44 GHz; modulation amplitude, 2.2 mT; gain, 1×10^5.

of these three waves infer a 1:1:1 stoichiometry of the constituent hemes. The 1.8-fold greater amplitude of the $g = 3.09$ wave as compared to the other waves agrees well with the theoretically deduced dependence of line intensity vs g factor, which predicts a ratio of 1.6 for the g factors under consideration (deVries & Albracht, 1979). The measured midpoint potentials are summarized in Table I.

Spectral Properties. Figure 3 shows g_z peaks observed under various different conditions on an expanded scale. It is evident that the position of the $g = 3.3$ line does not remain constant. More exact g values can be assigned to the three $g = 3.3$ hemes. This allows discrimination between different redox species and provides the basis for the determination of their orientations. The lowest potential heme (Figure 3b) exhibits the lowest g factor ($g = 3.29$).

The low-potential heme that can be selectively oxidized by low-temperature illumination (this is likely to be the +20-mV heme; see Discussion) permits its g factor to be determined rather accurately at $g = 3.31$ (Figure 3a). At 118 mV, both of these resolved low-potential hemes are oxidized, and accordingly the g value of the observed g_z line lies intermediate between the peak positions of the individual $E_m = -80$ mV ($g = 3.29$) and $E_m = +20$ mV ($g = 3.31$) species (Figure 3c). On oxidation of the +320-mV heme, a further displacement of the line toward lower magnetic fields is evident (Figure 3d). In addition, it is likely that a magnetic interaction occurs between the 320-mV heme and one or both of the low-potential hemes (see below). This interaction could influence the g factor of the hemes involved. Since a "pure" spectrum of the 320-mV heme has not been generated, the value of its g factor can only be estimated to be >3.32.

At very high potentials (Figure 3e), the oxidation of the 420-mV heme is reflected by a peak at $g = 3.09$. Due to the presence of ferricyanide in these samples, the g_y line is obscured by the large ferricyanide signal. However, in the oriented samples, the g_y absorption of this heme is clearly seen at $g = 2.23$ (see Orientation). No g_y line was detected for any of the other hemes.

In highly oxidized samples such as the one depicted in Figure 3e, an additional peak in between the $g = 3.3$ and the $g = 3.09$ line is seen. Measurements made under nonsaturating conditions for all the peaks indicate that the contribution of the middle peak to the spin concentration present in all signals is less than 5%. Therefore, it cannot represent an appreciable fraction of any of the four heme species.

Low-Temperature Illumination. (a) As mentioned already, illumination at 4 K of a fully reduced sample results in the appearance of a line at $g = 3.31$ (Figure 4a). At the same time, the signal at $g = 1.82$ is formed which is attributed to

the semiquinone iron, the terminal electron acceptor at this temperature (Prince et al., 1977). This cytochrome is stably oxidized as the line intensity is not diminished after the light is switched off. Warming the sample in the dark to >80 K induces a line shift to $g = 3.29$ (Figure 4a'). Further warming to room temperature presumably causes a recombination of the electron trapped at the acceptor side with the oxidized cytochrome because both the cytochrome and the semiquinone iron signals vanish.

From the g value, the heme photooxidized at 4 K seems to correspond to the +20-mV heme. However, since the g_z of the +320-mV heme in the redox titration may be influenced by a magnetic interaction with other oxidized hemes, we cannot strictly rule out that it is this heme which undergoes photooxidation at 4 K. This seems unlikely, however, when redox and distance factors are considered in light of the heme order arrived at under Discussion. The signal at $g = 3.29$ formed by warming in the dark can be confidently assigned to the −80-mV heme on the basis of its g value.

Thus, we assume that illumination at 4 K selectively oxidizes the +20-mV component while at higher temperatures an electron on the lowest potential heme can surmount an energy barrier to rereduce the low-temperature photooxidized heme.

(b) If the lowest potential heme is already oxidized prior to illumination, the peak photoinduced upon illuminating the sample at $T < 20$ K corresponds to a g value of about 3.31 and again is attributed to the +20-mV heme (Figure 4b). Warming to 100 K does not induce any spectral changes in this case. It is of note that the yield for photooxidation is much less than in (a) where almost 1 electron equiv of heme signal could be oxidized.

(c) At higher oxidation states, we observe no low-temperature photooxidation of low-spin hemes. However, at all redox states, illumination resulted in the formation of a small but clearly visible signal in the spectral region of high-spin hemes (Figure 4c). This photochemistry was stable only at $T < 30$ K; further warming completely reversed the spectral changes in this field region. As transition probabilities of $S = {}^5/_2$ hemes are drastically higher than for the low-spin configuration, the number of spins present in the high-spin form must be negligibly small compared to the proportion of $S = {}^1/_2$ hemes photooxidized as described in (a) and (b). Furthermore, the semiquinone iron signal did not increase. This might be due to the fact either that the amplitude of the corresponding semiquinone iron signal is below the threshold of detection or that the spectral changes in the $g = 6$ region do not represent photooxidation but instead are due to photolysis of axial heme ligands (Hori et al., 1982; Petrich et al., 1988). The latter explanation is consistent with the observation that the high-spin heme signal was not formed by chemical oxidation of the hemes.

Orientation. The orientation dependence of the observed peaks with respect to the membrane was studied in a range of redox states between fully oxidized and almost fully reduced. As there is a close correlation between the direction of g_z and the heme normal (Taylor, 1977; Mailer & Taylor, 1972; Hori, 1971), knowledge of the orientation of g_z is sufficient to determine the tilt angle of the heme plane with respect to the membrane. For clarity, only the data at two of these conditions are presented in detail:

(a) Spectra of the samples treated with low concentrations of dithionite only show the presence of a $g = 3.3$ line. The peak position changes with orientation of the multilayers, the g factor being minimal at 0° (Figure 5a). A plot of line intensity vs angle (Figure 5b) clearly indicates the presence

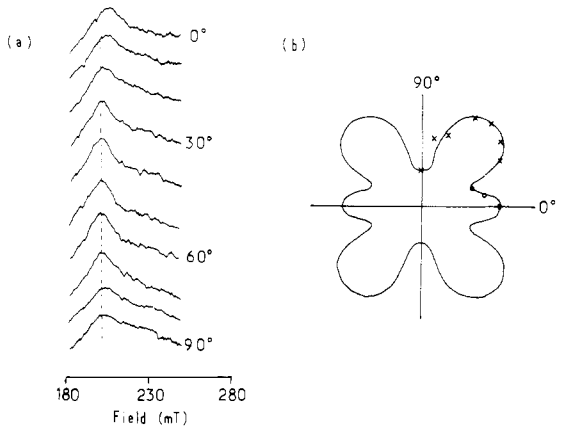

FIGURE 5: Orientation dependence in the g_z region as determined for the half-reduced state. Dilute sodium dithionite solution was applied to the oriented multilayers, leaving only the low-potential hemes oxidized. (a) Spectra taken at a range of orientations. Angles are given between the plane of the multilayer and the direction of the magnetic field. (b) Polar plot evaluation of (a). Crosses denote values obtained on the peak at the lower field position, whereas circles mark intensities of the peak shifted to higher field. EPR conditions are as described in Figure 1, except for the microwave power being 0.5 mW.

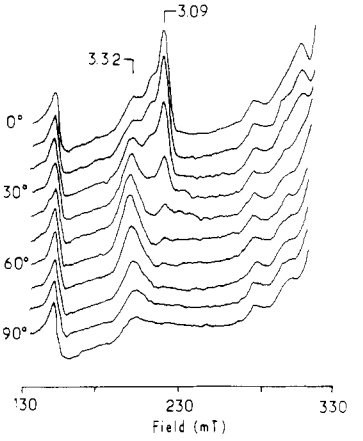

FIGURE 6: Orientation-dependent spectra recorded on the untreated multilayers. Angles are defined as in Figure 5. EPR conditions are as in Figure 5.

of two differently oriented hemes. The g_z direction of one of them is oriented at 45° whereas in the other species g_z is obviously parallel to the membrane. In the angular plot of Figure 5b, the values for the hemes at higher and lower g_z are distinguished by crosses and circles, respectively. Thus, the heme with g_z oriented at 0° (i.e., the heme plane is perpendicular to the membrane) displays the smaller g value, thereby being identified with the lowest potential heme. The +20-mV heme consequently lies at 45° to the membrane plane.

(b) Spectra of untreated membranes (Figure 6) contain additionally the peak of the 400-mV heme and extra intensity in the $g = 3.3$ region due to the presence of the +320-mV heme. In these conditions, the $g = 3.3$ peak shows a clear maximum at 45°. As the sample in Figure 5a is actually identical with the one in Figure 6 except for the reductant treatment, one can calculate differences between both sets of spectra. This subtraction of the orientation data with two hemes reduced from the data with all hemes oxidized yields the pure orientation of the 320-mV component. The angular dependence of these difference spectra is shown in Figure 7a. This heme is clearly oriented at 45°. By contrast, the $g = 3.09$ peak is maximal at 0°, inferring a perpendicular orientation of the heme (Figure 7b). In this sample also, the g_y absorption

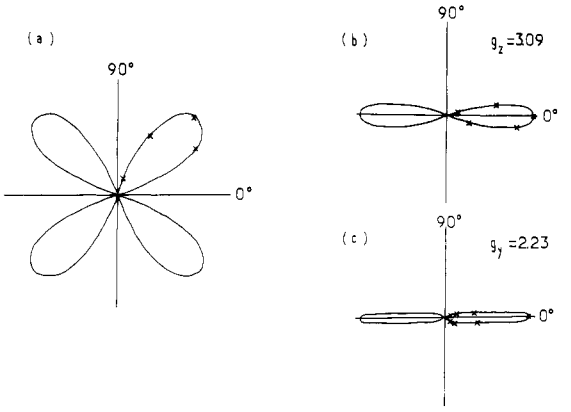

FIGURE 7: Polar plots of the line intensities as determined from Figures 6 and 5. (a) Plot of the intensity increment between the half-reduced (Figure 5) and untreated (i.e., highly oxidized) samples (Figure 6). (b and c) Plots of the intensities of the g_z = 3.09 and the g_y = 2.23 lines, respectively.

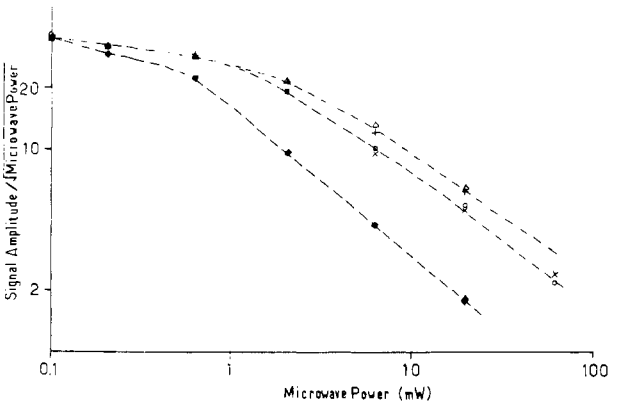

FIGURE 8: Comparison of the relaxation behavior of the heme subunit in its partially and fully oxidized states. The data points represent signal amplitudes of the g_z peaks, normalized at nonsaturating powers. Symbols are defined as follows: (×) one heme oxidized (−41 mV); (○) two hemes oxidized (+214 mV); (△) three hemes oxidized (+349 mV); (+ and ♦) all four hemes oxidized. (×, ○, △) and (+) denote values obtained on the g_z = 3.3 peak, whereas (♦) represents the g_z = 3.09 peak. EPR conditions: temperature, 8 K; modulation amplitude, 3.2 mT.

of the 400-mV heme is detected at g = 2.23 being highly oriented with maximal intensity parallel to the membrane plane (Figure 7c).

Examination of the orientation dependence of the $S = {}^5/_2$ signal reveals that the signal is actually made up of two peaks with slightly different positions and orientations. The line at g = 5.5 is oriented parallel to the membrane whereas the lower g-factor peak (g = 5.3) lies at 45° (data not shown). As in high-spin hemes both $g \approx 6$ directions are approximately parallel to the porphyrin plane, the species giving rise to this signal must be one of the hemes with the 45° tilt angle.

Isolated Reaction Centers. The dominant features in the spectra of oxidized isolated reaction centers are the two peaks at g = 3.3 and g = 3.09 as described above for the chromatophores. In some preparations, there was also an additional signal at g_z = 2.85 and g_y = 2.27 sometimes present at a significant amplitude. The intensities of this additional signal correlated with mistreatment of the preparation (i.e., a large signal was formed when samples were stored for long periods at −30 °C or repeatedly frozen and thawed or treated with the powerful oxidant potassium iridate). Obviously, solubilizing the reaction center destabilizes the native conformation of the hemes and increases the probability for occupancy of various conformational substates. The photoinduced spin ${}^5/_2$ signal could also be observed in reaction centers as could the small signal at g = 3.15.

Reaction center preparations lacking the g_z = 2.85, "damaged heme" signal were used to study the low-temperature photooxidation properties of samples poised at redox states where only the high-potential cytochromes are reduced, taking advantage of the low BChl content of these preparations. Nevertheless, no photooxidation of high-potential hemes at liquid helium temperatures was observable.

Power Saturation Properties. Figure 8 shows the dependence of line intensity vs microwave power determined for all four individual redox states.

The saturation characteristics are rather similar for the samples with only one and with two hemes oxidized. However, the peak is less readily saturated, when the 320-mV heme is additionally oxidized. The 400-mV heme relaxes much more slowly than all other hemes and may therefore be magnetically rather isolated.

Discussion

Redox Data. From early studies on the bound cytochrome subunit, the notion emerged that the four hemes contained in this protein subunit fall into two pairs of equivalent redox species, i.e., the low- and the high-potential hemes, respectively. More recently, optical studies on *Rps. viridis* provided evidence that actually all four cytochromes are inequivalent with respect to their midpoint potentials (Alegria & Dutton, 1988; Dracheva et al., 1986, 1988). While it was shown that all four hemes could be distinguished by their individual α peaks, the peak wavelengths proved to be too close to allow selective titrations to be done. Thus, discrimination within the two redox groups was mainly achieved by comparing single- to double-component Nernst fits to the data points. However, in this EPR study, the two high-potential components show up as two clearly distinct peaks (g_z = 3.3 and g_z = 3.09). The midpoint potential of each high-potential heme can therefore be determined without interference from the other species. Thus, our data independently demonstrate the redox heterogeneity of the high-potential hemes.

A less favorable situation exists for the low-potential pair where both hemes have similar EPR line positions. In this case, however, the titration of the peak shift provides rather clearcut evidence for the presence of two distinct low-potential cytochromes, and the comparison of one- and two-component fits further supports this result. For all four different redox species, the values obtained in this work (Table I) agree within 20 mV of the potentials reported by Dracheva et al. (1988). This allows a correlation of the EPR signals to the optical α maxima of the cytochromes (Table I). The E_m values provided by Alegria and Dutton (1988) are somewhat at variance with our values, but this work was done with isolated reaction centers in the form of monolayers deposited on glass from Langmuir–Blodgett films of reaction centers and the detergent laurylamine *N*-oxide. Thus, some differences compared to the native membranes might be expected. However, more recent redox titrations, coupled with spectroscopic analysis, done by Alegria and Dutton (unpublished results) on monolayers of reaction center preparations in which detergent was exchanged for phospholipid yield E_m values that are also within 20 mV of our numbers and spectral assignments similar to those of Dracheva et al. (1988).

Orientation. The assignment of heme tilt angles toward the membrane to individual redox species is shown in Table I. The main feature is that the highest and the lowest potential hemes are approximately perpendicular to the membrane whereas the two intermediate potential hemes are both tilted by about 45°. This finding is supported by LD studies (Alegria &

Dutton, 1987) which also show that the planes of the highest and the lowest potential hemes are at larger angles to the membrane than the intermediate potential cytochromes. Comparison of these orientations to the crystal structure implies that the two perpendicular species are the nearest and the furthest hemes with respect to the reaction center. Conversely, the intermediate potential hemes at an angle of 45° can be identified with the two middle hemes in the linear row of the cytochrome subunit.

The orientation data taken with the crystal structure provide an important structural limitation cutting down the number of possible configurations to four cases: (1) RC +400, +320, +20, and −80 mV; (2) RC +400, +20, +320, and −80 mV; (3) RC −80, +320, +20, and +400 mV; (4) RC −80, +20, +320, and +400 mV. Further restrictions on these models are described below.

The orientations determined in this work are rather different from the result obtained for the cytochrome subunit of *C. vinosum* which suggested two parallel chains each containing one low-potential cytochrome close to the reaction center and oriented parallel to the membrane in addition to one high-potential heme, further away and perpendicular to the membrane (Tiede et al., 1978). This discrepancy remains unresolved, and the cytochrome subunit from *C. vinosum* might indeed be structurally different from *Rps. viridis*; however, a reinvestigation of *C. vinosum* with the benefit of the analogy to *Rps. viridis* seems worthwhile.

For the 400-mV heme, the direction of the g_y line could also be determined. Theoretical treatments of low-spin heme structures predict correlation of the g_y direction to the plane of highest unpaired spin density (Taylor, 1977). However, the precise way in which protein structure affects the arrangement of the d orbitals of the iron has remained controversial. For myoglobins and hemoglobins, which are well studied by EPR, it was proposed that the direction of g_y is determined by the imidazole ring orientation of the proximal histidine in the fifth position (Helcké et al., 1968). The general applicability of this rule, however, was later criticized by Hori (1971) and Mailer and Taylor (1972). However, for the special case of histidine-methionine-liganded, soluble *c*-type cytochromes, a considerable amount of experimental evidence has accumulated, coming largely from NMR measurements, which indicates that in these systems the unpaired spin density is determined by the sixth methionine ligand rather than by the histidine in the fifth position (Senn et al., 1980; Mathews, 1985). According to these results, the direction of the lone pair orbital of the methionine sulfur is parallel to the iron d orbital containing the maximal unpaired spin density (Senn et al., 1980). For the case of horse heart ferricytochrome *c*, this is in excellent agreement with EPR results obtained on single crystals (Mailer & Taylor, 1972). Thus, if we assume that this correlation is correct, then a conformation with the lone pair orbital of the methionine sulfur lying parallel to the membrane (i.e., the methionine side chain close to but not exactly perpendicular with respect to the membrane) is predicted for the +400-mV heme by our results.

Unfortunately, the g_y lines of the remaining two histidine-methionine hemes are not detectable in our system. However, in principle, it should be possible to determine these directions by EPR measurements on single crystals of the *Rps. viridis* reaction center.

Low-Temperature Photochemistry. As described above, low-temperature illumination of samples having the cytochrome complement fully reduced results in photooxidation of what is probably the +20-mV heme. Upon warming, this heme is then rereduced by electron transfer from the −80-mV heme. We interpret this observation as an indication that the −80-mV heme is further away from the special pair than is the photooxidized heme. This finding, taken together with the structural restrictions imposed by the orientation, puts the −80-mV heme at the end of the row of hemes, distal to the reaction center. As a consequence, the 400-mV heme must be positioned next to the reaction center. Placing the highest potential cytochrome closer to the reaction center than the +320-mV heme is also supported by optical data on the rereduction kinetics of the oxidized special pair BChl (Dracheva et al., 1986, 1988; Shopes et al., 1987) and by voltage measurements (Dracheva et al., 1987, 1988).

These arguments reduce the number of heme configurations in the cytochrome subunit to two possibilities: (1) RC +400, +320, +20, and −80 mV; or (2) RC +400, +20, +320, and −80 mV. This leaves ambiguous only the positioning of the +20-mV and the +320-mV species in the middle of the array.

Magnetic Interactions. Straightforward interpretation of the data on relaxation rates of the four hemes is hampered by the overlap of g_z peaks of all except the highest potential heme. A superposition of the relaxation behavior of these three hemes is observed, and a deconvolution into the individual components is not possible.

Accordingly, we cannot distinguish between two possible situations. (a) All hemes are magnetically isolated, implying the following order of relaxation rates: $(1/T)_{+400mV} < (1/T)_{-80mV} = (1/T)_{+20mV} < (1/T)_{+320mV}$. (b) The two low-potential hemes are magnetically isolated from each other; however, the +320-mV component, when oxidized, magnetically interacts with one or both of the low-potential hemes, causing a net increase in the rate of relaxation of the peak at $g = 3.3$.

In the *C. vinosum* system, the g_z peaks of the high-potential hemes do not overlap with the low-potential hemes, and the various interactions can be directly monitored (Tiede et al., 1978). The results reported with *C. vinosum* correspond to situation (b). If we consider then that a magnetic interaction does occur between the hemes in *Rps. viridis*, we can attempt to distinguish between the two possible heme orders arrived at above by taking into account the interheme Fe–Fe distances obtained from the X-ray structure (i.e., RC heme ← 14 Å → heme ← 16 Å → heme ← 14 Å → heme). The magnetic interaction effects as described earlier are consistent with the following heme order: RC +400 mV, +20 mV, +320 mV, −80 mV. This configuration, with the +320-mV heme being between the two low-potential hemes, would explain not only the apparent lack of interaction between the +20-mV and the −80-mV species but also the proposed interaction between the +320-mV heme and either or both of the low-potential hemes. The alternative heme order (RC +400 mV, +320 mV, +20 mV, −80 mV) is much less reasonable since it requires that the proposed interaction occurs over the 16-Å distance between the +320-mV and +20-mV hemes while no interaction occurs between the +20-mV and −80-mV hemes at a distance of only 14 Å.

Relationship between Spectral and Structural Properties. According to the crystal structure of the *Rps. viridis* reaction center, three of the four hemes are coordinated by histidine and methionine in fifth and sixth positions, whereas the second heme from the reaction center has two histidines as axial ligands (Weyer et al., 1987). The same pattern of three hemes with the same g_z peak and one heme at a different position reappears in the EPR spectra. However, according to our analysis, the obvious correlation between these observations

does not hold: the two-histidine-liganded heme is one of the three hemes displaying a $g_z = 3.3$ peak, whereas the spectrally different heme is identified as one of the three His-Met-liganded hemes.

Usually bisimidazole-coordinated hemes show g values in the range of 2.9–3.1, but there are also exceptions to this rule. For example, a large amount of evidence supports the notion that the *b* cytochromes in cytochrome *bc* complexes are His-His-coordinated (Widger et al., 1984; Salerno, 1984), but, nevertheless, they show g_z factors as high as 3.6–3.8. This can be rationalized by assuming a mutually perpendicular conformation for the planes of the two histidines liganding these hemes. Thereby the rhombic distortion of the crystal field is lowered and a larger admixture of orbital motion is allowed for (Palmer, 1985; Salerno, 1984). Thus, we would predict from our data that the two imidazole ring planes in the bis-histidine heme (i.e., probably the +20-mV heme) of the cytochrome subunit are twisted relative to each other and are not in the relaxed, fully parallel configuration.

In general, histidine-methionine-liganded hemes exhibit g_z factors ranging from 2.9 to 3.5. Even in the rather homologous family of the soluble cytochromes *c*, g_z values range from 3.0 to 3.3 (Palmer, 1985), and thus our results on the His-Met species can easily be accommodated within this framework. To our knowledge, the structural factors determining the rhombic and tetragonal splitting parameters (and therefore influencing the g factors) in His-Met compounds are not well understood. Again, single-crystal EPR studies on the cytochrome subunit of *Rps. viridis* could provide a lot of useful information pertinent to this question.

Models. As discussed above, our orientation and electron-transfer results allow the number of possible arrangements to be limited to model 1 (RC +400, +320, +20, and −80 mV) and model 2 (RC +400, +20, +320, and −80 mV). Of the two models, our magnetic relaxation data are best accommodated in model 2.

There are two further aspects in favor of model 2: (a) The two-histidine-liganded heme, second from the RC (Weyer et al., 1987), belongs to a class of *c*-type cytochromes that tend to be low potential. Although this is not a stringent argument, it would be in conflict with model 1. (b) Recently from a comparison of low-temperature LD-optical spectroscopy on oriented reaction centers with calculations based on the crystal structure, it is concluded that the third heme from the reaction center was probably the +320-mV component (A. Vermeglio, P. Richaud, and J. Breton, unpublished results). This does not fit with model 1. Taking all these additional factors into account, we strongly favor model 2.

Under Results, it is stated that the heme photooxidized at 4 K could possibly be the +320-mV component. From the final heme order, this seems unlikely. It is much more likely that the positive charge would be stable at 4 K on the electrochemically more favorable +20-mV heme, which is closer to the reaction center. The thermal barrier to further electron transfer from the −80-mV heme can be rationalized in terms of the interposition of the +320-mV heme.

The peculiar arrangement in model 2 with its alternating sequence of high- and low-potential hemes raises a number of questions with respect to the mechanism of electron transport in this system, which still are far from being fully answered. However, it should be kept in mind that due to the close proximity of the hemes in this protein, mutual influences on the redox properties seem highly probable [for a discussion, see Dutton (1986)]. Indeed, some of the phenomena observed with the low-temperature photooxidation can probably be explained by models which take electrostatic interactions into account [see, for example, the work with cytochrome c_3 by Santos et al. (1984)].

ACKNOWLEDGMENTS

We thank Drs. Alegria and Dutton and Drs. Vermeglio, Richault, and Breton for useful discussion and for providing us with preprints of their work. Thanks are also due to Dr. M. Denis for a kind gift of porphyrexide and to S. Andrian-ambinintsoa for growth and maintenance of the bacterial cultures and for isolating the reaction centers. We would further like to thank Drs. Michel and Deisenhofer for providing the coordinates of the reaction center chromophores and Dr. H. H. Robinson for stimulating discussion.

REFERENCES

Alegria, G., & Dutton, P. L. (1987) in *Cytochrome Systems* (Papa, S., Chance, B., & Ernster, L., Eds.) pp 601–608, Plenum Press, New York and London.

Alegria, G., & Dutton, P. L. (1988) *Biophys. J. 53*, 615a.

Blasie, J. K., Erecinska, M., Samuels, S., & Leigh, J. S. (1978) *Biochim. Biophys. Acta 501*, 33–52.

Case, C. D., & Parson, W. W. (1973) *Biochim. Biophys. Acta 325*, 441–453.

Clayton, R. K., & Clayton, B. J. (1978) *Biochim. Biophys. Acta 501*, 478–487.

Cohen-Bazire, G., Sistrom, W. R., & Stanier, R. Y. (1957) *J. Cell. Comp. Physiol. 49*, 25–68.

Deisenhofer, J., Epp, O., Miki, K., Huber, R., & Michel, H. (1984) *J. Mol. Biol. 180*, 385–398.

DeVault, D., & Chance, B. (1966) *Biophys. J. 6*, 825–847.

deVries, S., & Albracht, S. P. J. (1979) *Biochim. Biophys. Acta 546*, 334–340.

Dracheva, S. M., Drachev, L. A., Zaberezhnaya, S. M., Konstantinov, A. A., Semenov, A. Y., & Skulachev, V. P. (1986) *FEBS Lett. 205*, 41–46.

Dracheva, S. M., Drachev, L. A., Konstantinov, A. A., Semenov, A. Y., Skulachev, V. P., Arutjunjan, A. M., Shuvalov, V. A., & Zaberezhnaya, S. M. (1988) *Eur. J. Biochem. 171*, 253–264.

Dutton, P. L. (1971) *Biochim. Biophys. Acta 226*, 63–80.

Dutton, P. L. (1986) *Encycl. Plant Physiol., New Ser. 19*, 197–237.

Dutton, P. L., & Prince, R. (1978) in *The Photosynthetic Bacteria* (Clayton, R. K., & Sistrom, W. R., Eds.) pp 525–570, Plenum Press, New York and London.

Helckē, G. A., Ingram, D. J. E., & Slade, E. F. (1968) *Proc. R. Soc. London, Ser. V 169*, 275–288.

Hori, H. (1971) *Biochim. Biophys. Acta 251*, 227–235.

Hori, H., Ikeda-Saito, M., Leigh, J. S., Jr., & Yonetani, T. (1982) *Biochemistry 21*, 1431–1437.

Mailer, C., & Taylor, C. P. S. (1972) *Can. J. Biochem. 50*, 1048–1105.

Mathews, F. S. (1985) *Prog. Biophys. Mol. Biol. 45*, 1–56.

Nitschke, W., & Rutherford, A. W. (1988) *VIth International Symposium on Photosynthetic Prokaryotes*, Noordwijkerhout, The Netherlands, Abstr. 35.

Palmer, G. (1985) *Biochem. Soc. Trans. 13*, 548–560.

Petrich, J. W., Poyart, C., & Martin, J. L. (1988) *Biochemistry 27*, 4049–4060.

Prince, R. C., Tiede, D. M., Thornber, J. P., & Dutton, P. L. (1977) *Biochim. Biophys. Acta 462*, 467–490.

Prince, R. C., Tiede, D. M., Leigh, J. S., & Dutton, P. L. (1978) *6th International Biophysics Congress*, Kyoto, Japan, Abstr. V-25-(510).

Rutherford, A. W. (1979) Ph.D. Thesis, University of London.

Salerno, J. S. (1984) *J. Biol. Chem. 259*, 2331-2336.
Santos, H., Moura, J. J. G., Moura, I., LeGall, J., & Xavier, A. V. (1984) *Eur. J. Biochem. 141*, 283-296.
Seibert, M., & DeVault, D. (1970) *Biochim. Biophys. Acta 205*, 200-231.
Senn, H., Keller, R. M., & Wüthrich, K. (1980) *Biochem. Biophys. Res. Commun. 92*, 1362-1369.
Shill, D. A., & Wood, P. M. (1984) *Biochim. Biophys. Acta 764*, 1-7.
Shopes, R. J., Levine, L. M. A., Holten, D., & Wraight, C. A. (1987) *Photosynth. Res. 12*, 165-180.
Skulachev, V. P., Drachev, L. A., Dracheva, S. M., Konstantinov, A. A., Semenov, A. Y., & Shuvalov, V. A. (1987) in *Cytochrome Systems* (Papa, S., Chance, B., & Ernster, L., Eds.) pp 609-616, Plenum Press, New York and London.
Taylor, C. P. S. (1977) *Biochim. Biophys. Acta 491*, 137-149.
Tiede, D. M., Leigh, J. S., & Dutton, P. L. (1978) *Biochim. Biophys. Acta 503*, 524-544.
Weyer, K. A., Lottspeich, F., Gruenberg, H., Lang, F., Oesterheld, D., & Michel, H. (1987) *EMBO J. 6*, 2197-2202.
Widger, W. R., Cramer, W. A., Herrmann, R. G., & Trebst, A. (1984) *Proc. Natl. Acad. Sci. U.S.A. 81*, 674-678.

Synthesis, Location, and Lateral Mobility of Fluorescently Labeled Ubiquinone 10 in Mitochondrial and Artificial Membranes†

K. Rajarathnam,‡ J. Hochman,§ M. Schindler, and S. Ferguson-Miller*
Department of Biochemistry, Michigan State University, East Lansing, Michigan 48824
Received September 13, 1988; Revised Manuscript Received December 20, 1988

ABSTRACT: To explore the influence of the long isoprene chain of ubiquinone 10 (UQ) on the mobility of the molecule in a phospholipid bilayer, we have synthesized a fluorescent derivative of the head-group moiety of UQ and measured its lateral diffusion in inner membranes of giant mitochondria and in large unilamellar vesicles. The diffusion coefficients, determined by the technique of fluorescence redistribution after photobleaching, were 3.1×10^{-9} cm^2 s^{-1} in mitochondria and 1.1×10^{-8} cm^2 s^{-1} in vesicles. Similar diffusion rates were observed for fluorescently labeled phosphatidylethanolamine (PE) with the same moiety attached to its head group (4-nitro-2,1,3-benzooxadiazole: NBD). Fluorescence emission studies carried out in organic solvents of different dielectric constants, and in vesicles and mitochondrial membranes, indicate that NBDUQ is located in a more hydrophobic environment than NBDPE or the starting material IANBD (4-[*N*-[(iodoacetoxy)ethyl]-*N*-methylamino]-7-nitro-2,1,3-benzoxadiazole). Fluorescence quenching studies carried out with $CuSO_4$, a water-soluble quenching agent, also indicate that NBDUQ is located deeper in the membrane than NBDPE. These results suggest that ubiquinone and PE are oriented differently in a membrane, even though their diffusion rates are similar. Conclusions regarding whether or not diffusion of UQ is a rate-limiting step in electron transfer must await a more detailed knowledge of the structural organization and properties of the electron transfer components.

Ubiquinone 10 (UQ)[1] is an integral component of the electron transfer chain that mediates the transfer of electrons between respiratory complexes in the inner mitochondrial membrane and participates in the translocation of protons across the membrane. A hydrophobic molecule with a long, somewhat rigid, isoprenoid side chain of 50 Å, UQ in an extended form would span the bilayer (Trumpower, 1981). It was originally proposed by Green (1962) that UQ could act as a mobile electron carrier, because of its structure and presence in excess over its redox partners (about 20-fold molar excess over cytochrome bc_1; Capaldi, 1982). It has become increasingly evident that diffusion of UQ is important for electron transfer, but whether its diffusion is rate limiting remains to be established. To gain insight into this question, it is important to know the diffusion rates of UQ, the activation energy for the diffusion process compared to that of the electron transfer process, the K_m values for the interaction of native quinone with the electron transfer complexes in the mitochondrial membrane, and the average distance UQ has to diffuse to accomplish electron transfer. Currently, there is controversy regarding all these values.

Gupte et al. (1984) have measured the diffusion of a fluorescent derivative of a ubiquinone analogue which has an alkyl side chain corresponding in length to only two isoprene units. The lateral diffusion coefficients they determined by fluorescence redistribution after photobleaching (FRAP) were 3×10^{-9} cm^2 s^{-1} in the mitochondrial membranes and 5.5×10^{-8} cm^2 s^{-1} in phospholipid vesicles (Hackenbrock et al., 1986a). From diffusion measurements as a function of temperature (Hackenbrock et al., 1986b) and as a function of

† This work was supported by NIH Grant GM26916 (S.F.-M.).
* To whom correspondence should be addressed.
‡ Present address: Department of Chemistry, University of California Davis, Davis, CA 95616.
§ Present address: INTERx Research Corp., 2201 W. 21st St., Lawrence, KS 66046.

[1] Abbreviations: BSA, bovine serum albumin; CCCP, carbonyl cyanide *m*-chlorophenylhydrazine; UQ, coenzyme Q_{10}, ubiquinone 10; DMAP, (dimethylamino)pyridine; IANBD, 4-[*N*-[(iodoacetoxy)ethyl]-*N*-methylamino]-7-nitro-2,1,3-benzoxadiazole; NBDUQ, 4-[*N*-(acetoxyethyl)-*N*-methylamino]-7-nitro-2,1,3-benzoxadiazole–ubiquinone 10; NBDPE, *N*-(7-nitro-2,1,3-benzoxadiazol-4-yl)dipalmitoylphosphatidylethanolamine; THF, tetrahydrofuran; Thiolyte, monobromobimane; TLC, thin-layer chromatography.

0006-2960/89/0428-3168$01.50/0